0022-3565/09/3281-351–361
THE JOURNAL OF PHARMACOLOGY AND EXPERIMENTAL THERAPEUTICS
U.S. Government work not protected by U.S. copyright
JPET 328:351–361, 2009

Vol. 328, No. 1
144717/3420297
Printed in U.S.A.

The Endogenous Brain Constituent *N*-Arachidonoyl L-Serine Is an Activator of Large Conductance Ca^{2+}-Activated K^+ Channels

Grzegorz Godlewski, László Offertáler, Douglas Osei-Hyiaman, Fong Ming Mo, Judith Harvey-White, Jie Liu, Margaret I. Davis, Li Zhang, Raj K. Razdan, Garry Milman, Pal Pacher, Partha Mukhopadhyay, David M. Lovinger, and George Kunos

Laboratories of Physiologic Studies (G.G., L.O., D.O.-H., F.M.M., J.H.-W., J.L., P.P., P.M., G.K.) and Integrative Neuroscience (M.I.D., L.Z., D.M.L.), National Institute on Alcohol Abuse and Alcoholism, National Institutes of Health, Bethesda, Maryland; Organix, Inc., Woburn, Massachusetts (R.K.R.); and Department of Medicinal Chemistry, Hebrew University, Jerusalem, Israel (G.M.)

Received August 11, 2008; accepted October 7, 2008

ABSTRACT

The novel endocannabinoid-like lipid *N*-arachidonoyl L-serine (ARA-S) causes vasodilation through both endothelium-dependent and -independent mechanisms. We have analyzed the vasorelaxant effect of ARA-S in isolated vascular preparations and its effects on Ca^{2+}-activated K^+ currents in human embryonic kidney cells stably transfected with the α-subunit of the human, large conductance Ca^+-activated K^+ (BK_{Ca}) channel [human embryonic kidney (HEK) 293hSlo cells]. ARA-S caused relaxation of rat isolated, intact and denuded, small mesenteric arteries preconstricted with (*R*)-(−)-1-(3-hydroxyphenyl)-2-methylaminoethanol hydrochloride (pEC_{50}, 5.49 and 5.14, respectively), whereas it caused further contraction of vessels preconstricted with KCl (pEC_{50}, 5.48 and 4.82, respectively). Vasorelaxation by ARA-S was inhibited by 100 nM iberiotoxin. In human embryonic kidney cells stably transfected with the α-subunit of the human BK_{Ca} channel cells, ARA-S and its enantiomer, *N*-arachidonoyl-D-serine, enhanced the whole-cell outward K^+ current with similar potency (pEC_{50}, 5.63 and 5.32, respectively). The potentiation was not altered by the β_1 subunit or mediated by ARA-S metabolites, stimulation of known cannabinoid receptors, G proteins, protein kinases, or Ca^{2+}-dependent processes; it was lost after patch excision or after membrane cholesterol depletion but was restored after cholesterol reconstitution. BK_{Ca} currents were also enhanced by *N*-arachidonoyl ethanolamide (pEC_{50}, 5.27) but inhibited by another endocannabinoid, *O*-arachidonoyl ethanolamine (pIC_{50}, 6.35), or by the synthetic cannabinoid O-1918 [(−)-1,3-dimethoxy-2-(3-3,4-*trans*-*p*-menthadien-(1,8)-yl)-orcinol] (pIC_{50}, 6.59), which blocks ARA-S-induced vasodilation. We conclude the following. 1) ARA-S directly activates BK_{Ca} channels. 2) This interaction does not involve cannabinoid receptors or cytosolic factors but is dependent on the presence of membrane cholesterol. 3) Direct BK_{Ca} channel activation probably contributes to the endothelium-independent component of ARA-S-induced mesenteric vasorelaxation. 4) O-1918 is a BK_{Ca} channel inhibitor.

Endocannabinoids are endogenous fatty acid derivatives that bind to and activate the same receptors that recognize the plant-derived cannabinoid Δ^9-tetrahydrocannabinol (Pacher et al., 2006). Two $G_{i/o}$-protein coupled cannabinoid receptors have been identified so far: the brain-type or CB_1 receptor, present at high levels in the brain and at lower levels in the peripheral tissues, and the CB_2 receptor, largely confined to immune and hematopoietic cells (Howlett, 2005). In addition to their well known neurobehavioral effects, cannabinoids and their endogenous counterparts can influence other

This study was supported in part by the Intramural Research Program of the National Institutes of Health, National Institute on Alcohol Abuse and Alcoholism.

Article, publication date, and citation information can be found at http://jpet.aspetjournals.org.

doi:10.1124/jpet.108.144717.

ABBREVIATIONS: CB, cannabinoid; anandamide, *N*-arachidonoyl ethanolamide; TRPV, transient receptor potential vanilloid; ARA-S, *N*-arachidonoyl L-serine; BK_{Ca}, large conductance Ca^+-activated K^+; O-1918, (−)-1,3-dimethoxy-2-(3–3,4-*trans*-*p*-menthadien-(1,8)-yl)-orcinol; virodhamine, *O*-arachidonoyl ethanolamine; HEK, human embryonic kidney; HEK293hSlo, human embryonic kidney cells stably transfected with the α-subunit of the human BK_{Ca} channel; DMEM, Dulbecco's modified Eagle's medium; ES, external solution; IS, internal solution; BAPTA, 1,2-bis(2-aminophenoxy)ethane-*N*,*N*,*N*′,*N*′-tetraacetic acid; 2-AG, 2-arachidonoyl glycerol; 11,12-EET, (±)11(12)-epoxy 5*Z*,8*Z*,14*Z*-eicosatrienoic acid; NS 1619, 1,3-dihydro-1-[2-hydroxy-5-(trifluoromethyl)phenyl]-5-(trifluoromethyl)-2*H*-benzimidazol-2-one; PI(4,5)P_2, L-α-phosphatidyl-D-*myo*-inositol-4,5-bisphosphate triammonium salt; RT, reverse transcriptase; PCR, polymerase chain reaction; rapamycin, 23,27-epoxy-3*H*-pyrido[2,1-*c*][1,4]oxaazacyclohentriacontine; URB597, (3′-aminocarbonyl)[1,1′-biphenyl]-3-yl)-cyclohexylcarbamate; 14,15-EEZE, 14,15-epoxyeicosa-5(*Z*)-enoic acid; indomethacin, 1-(4-chlorobenzoyl)-5-methoxy-2-methyl-3-indoleacetic acid; NDGA, nordihydroguaiaretic acid; phenylephrine, (*R*)-(−)-1-(3-hydroxyphenyl)-2-methylaminoethanol hydrochloride; GDP-β-S, guanosine 5′-[β-thio]diphosphate; NP_o, open probability of *n* channels; HEK293hSloβ_1, HEK293hSlo cells cotransfected with β_1 subunit.

physiological functions, including cardiovascular variables. In anesthetized animals, the endocannabinoid-arachidonoyl ethanolamide (anandamide) elicits hypotension primarily through CB_1 receptor-mediated cardiodepression (Bátkai et al., 2004). Anandamide also interacts with transient receptor potential vanilloid (TRPV) 1 receptors, although with a potency less than its potency at CB_1 receptors (Zygmunt et al., 1999). In certain vascular beds, anandamide causes vasodilation, which does not involve activation of CB_1, CB_2, or TRPV1 receptors and has both endothelium-dependent and -independent components, the sensitivity of the former to pertussis toxin suggesting the involvement of a putative G_i/G_o-coupled receptor. The term "abnormal cannabidiol-sensitive receptor" has been coined, based on the similar vasodilator effect of this atypical synthetic cannabinoid ligand, which is not recognized by CB_1, CB_2, or TRPV1 receptors (Járai et al., 1999).

N-Arachidonoyl L-serine (ARA-S) is a novel, endogenous lipoamino acid present in the brain (Milman et al., 2006), which can modulate neuronal-type Ca^{2+} channels (Guo et al., 2008). Chemically, ARA-S resembles anandamide but has no or very low affinity for CB_1, CB_2, or TRPV1 receptors. On the other hand, ARA-S induces vasodilation in rat isolated mesenteric arteries and aorta, which, similarly to the effects of anandamide or abnormal cannabidiol, has endothelium-dependent and -independent components (Milman et al., 2006).

The endothelium-independent, pertussis toxin-resistant component of the vasodilator effect of anandamide has been linked to activation of the large conductance, calcium-activated potassium (BK_{Ca}) channel present in vascular smooth muscle (Plane et al., 1997), independently of CB_1, CB_2, or TRPV1 receptors or anandamide metabolism (White et al., 2001). An electrophysiological study of anandamide-induced BK_{Ca} currents suggests their dependence on undefined cytoplasmic factor(s) (Sade et al., 2006). In blood vessels, BK_{Ca} channels are expressed primarily in the smooth muscle cells, where they regulate vascular tone in response to changes in membrane potential, neurotransmitters, and cytosolic factors, e.g., calcium, protein kinases, and endothelium-derived hyperpolarizing factors (Brenner et al., 2000; Ghatta et al., 2006; Lu et al., 2006).

We tested the hypothesis that ARA-S relaxes isolated rat mesenteric arteries by activating BK_{Ca} channels. We also examined this mechanism in cells heterologously expressing the human BK_{Ca} channel. Our findings indicate that ARA-S activates BK_{Ca} channels, which likely accounts for its endothelium-independent vasorelaxant effect. In addition, we found the structural anandamide analog, *O*-arachidonoyl ethanolamine (virodhamine), and the atypical synthetic cannabinoid, O-1918, to be potent BK_{Ca} channel inhibitors.

Materials and Methods

Vasomotor Response in Rat Isolated Mesenteric Arteries. Third-order segments of mesenteric arteries (200–300 μm in diameter) were isolated from male Sprague-Dawley rats (200–300 g) and mounted in a wire myograph (Kent Scientific Corporation, Litchfield, CT), as described previously (Begg et al., 2003). Concentration-response curves were constructed by cumulative addition of ARA-S to vessels precontracted with 5 μM phenylephrine or 60 mM KCl. The functional integrity of the endothelium was verified by >90% relaxation elicited by 10 μM acetylcholine. The endothelium was denuded by rubbing the inside of the artery with the mounting wire, resulting in the loss of acetylcholine-induced relaxation. Some vessels were pretreated with 100 nM iberiotoxin for 20 min before the experiment.

Cell Culture. Human embryonic kidney (HEK) 293 cells were from the American Type Culture Collection (Manassas, VA). HEK293 cells stably transfected with the cDNA encoding human BK_{Ca} channel α-subunit splice variant, hbr1, derived from brain (HEK293hSlo) (Martin et al., 2004) were generously provided by Dr. Steven Treistman (University of Massachusetts, Worcester, MA). HEK293 cells were grown as monolayers on 25-cm^2 culture flasks in L-glutamine (292 μg/ml), D-glucose (4.5 mg/ml), and sodium pyruvate (110 μg/ml)-enriched Dulbecco's modified Eagle's medium (DMEM; Invitrogen, Carlsbad, CA) containing 10% heat-inactivated fetal bovine serum, penicillin (100 IU/ml), and streptomycin (100 μg/ml; Invitrogen). Selective pressure in HEK293hSlo cells was maintained by the presence of Geneticin (G-418, 500 μg/ml; Invitrogen) in the medium. All cells were cultured at 37°C under a humidified atmosphere of 5% CO_2. On the day of the experiment, cells were subcultured onto 35-mm plastic dishes and were allowed to adhere for 4 h before use. Before patch-clamp recording, the medium was replaced with external solution (ES).

Patch Clamp. Experiments were performed as described earlier (Begg et al., 2003), with modifications. Recording electrodes were pulled from borosilicate capillaries (TW150F-4; World Precision Instruments, Inc., Sarasota, FL) and fire polished to give resistances of 1.5 to 2.5 MΩ (whole-cell mode and isolated outside-out patches) or 8 to 15 MΩ (cell-attached mode). In whole cells and isolated outside-out patches, the electrodes were backfilled with internal solution (IS) of the following composition: 50 mM KCl, 70 mM KAsp, 8 mM NaCl, 1 mM $MgCl_2$, 2 mM MgATP, 0.3 mM NaGTP, and 10 mM HEPES (adjusted to pH 7.2 with KOH; osmolarity, 305–315 mOsm/l). Unless stated otherwise, free intracellular calcium concentration ($[Ca^{2+}]_i$) was clamped at 1 μM with 0.01 M 1,2-bis(2-aminophenoxy)ethane-*N*,*N*,*N*′,*N*′-tetraacetic acid (BAPTA) mixed with the appropriate amount of $CaCl_2$. The composition of ES was as follows: 135 mM NaCl, 2.5 mM KCl, 1.0 mM $MgCl_2$, 10 mM HEPES, 10 mM glucose, and 2.5 mM $CaCl_2$ (adjusted to pH 7.4 with NaOH; osmolarity, 340–350 mOsm/l). For single-channel recordings in the cell-attached mode, both ES and IS solutions contained 140 mM KCl, 2.5 mM $CaCl_2$, 1 mM $MgCl_2$, 10 mM HEPES, and 10 mM glucose, pH 7.4 (osmolarity, 340–350 mOsm/l). Chloride-coated silver wires connected the pipette IS to the probe input. The probe of the patch amplifier (Axopatch 1D; Axon Instruments) was mounted on a manipulator and connected through a digital interface (Digidata 1320A, Molecular Devices, Sunnyvale, CA) to a computer. The output signals were filtered with an eight-pole low-pass Bessel filter at 2 kHz (whole cells and isolated patches) or 3 kH (cell-attached mode) and digitized at 40 KHz. pCLAMP 9.1 software (Molecular Devices) was used for data acquisition and for off-line data analysis. All experiments were performed at room temperature.

Membrane currents were measured after Gigaseal formation (cell-attached mode) and disruption of the cell membrane (whole-cell mode) or excision of membrane patches (outside-out patch mode). This process was monitored by applying a test pulse (5 mV, 5 ms, 100 Hz) to the cell, which allowed the analysis of series resistance and cancellation of capacitive transients. Cells were voltage clamped at a holding potential of −60 mV (whole-cell mode and isolated outside-out patches), or extracellular membrane potential of +40 mV was applied (cell-attached mode). A series of depolarizing steps was generated in 10-mV increments to determine the conductance and current-voltage relationships. To test the effect of virodhamine and O-1918, the outward current was generated by a single 90-mV step in cells preincubated with ligands or their vehicles. To test the effect of ARA-S, anandamide, 2-arachidonoyl glycerol (2-AG), (±)11(12)-epoxy 5*Z*,8*Z*,14*Z*-eixosatrienoic acid (11,12-EET), and the BK_{Ca} activator, NS 1619, on the BK_{Ca} current, a single voltage step from the holding potential was applied before and after the application of the ligand or its vehicle. In preliminary experiments, each ligand was

applied on the cell surface at the concentration of 3 or 10 μM to establish the time course of drug action. The maximally effective exposure periods are provided in legends to the figures. The voltage step represented 20% of the peak current amplitude observed at +60 mV (I_{max}) or 20% of the maximal conductance (G_{max}). The latter approach was used only when ARA-S was examined in the presence of ligands affecting the BK_{Ca} channel current by themselves. For tail current analysis, a single test pulse of +100 mV was applied, followed by increasing hyperpolarizing steps from +30 to −170 mV in 10-mV increments.

Transient Transfection. HEK293hSlo cells were grown to 80 to 90% confluence in 35-mm Falcon tissue culture dishes coated with poly-D-lysine. Transient transfection was performed using the Lipofectamine 2000 reagent (Invitrogen) according to the manufacturer's instruction. In brief, 2 μl of Lipofectamine 2000 was mixed together with ~1 μg of plasmid cDNA in 1 ml of serum-free minimal essential medium supplemented with L-glutamine and 4.5 g/l D-glucose (Invitrogen) and placed for 4 h in a humidified incubator containing 5% CO_2 at 37°C. DNA-containing medium was then aspirated and replaced with the regular cell culture medium. Electrophysiological recordings were typically performed 2 to 3 days after transfection. The blue light was used to excite green fluorescent protein to find transfected cells.

The plasmid construct containing the human β_1 subunit was generously provided by Dr. Steven Treistman (University of Massachusetts). The fusion constructs used for membrane L-*a*-phosphatidyl-D-*myo*-inositol-4,5-bisphosphate triammonium salt [$PI(4,5)P_2$] depletion were kindly provided by Dr. Tamas Balla (National Institute of Child Health and Human Development, National Institutes of Health, Bethesda, MD).

Reverse Transcriptase-Polymerase Chain Reaction Analysis. Total RNA was isolated from cultured cells using TRIzol (Invitrogen) and then purified using RNase-free DNase with the RNeasy Set (QIAGEN, Valencia, CA). Purified RNA was reverse-transcribed (RT) with the SuperScript First-Strand Synthesis System (Invitrogen). The resulting single-stranded cDNA was denatured for 2 min at 95°C and then subjected to 35 cycles of amplification, each consisting of 30 s at 95°C, followed by 30 s at 55°C and 3 min at 72°C, with a final 10-min extension step at 72°C during the last cycle. Fifty microliters of polymerase chain reaction (PCR) mixture contained the cDNA template (1 μg), primer pair (each 1 μM), and components of PCR SuperMix High Fidelity (45 μl) (Invitrogen). The following forward versus reverse primer was designed to amplify a 259-bp segment of the human BK_{Ca} channel α-subunit mRNA: 5′-ATATCCGCCCAGACACTGAC-3′ versus 5′-GCACCGTGAAGAAATCCACT-3′. The human β-actin gene was amplified as a control. The PCR products were separated by electrophoresis on a 0.9% agarose gel (Invitrogen) in the presence of an 80- to 1000-bp DNA ladder (MBI Fermentas, Hanover, MD). RNA without reverse transcriptions did not yield any amplicons, indicating the absence of genomic DNA contamination.

Membrane Cholesterol Depletion and Repletion. Experiments were performed as described earlier (Westover et al., 2003). In brief, HEK293hSlo cells were grown to subconfluence in 60-mm polystyrene culture dishes coated with poly-D-lysine. For cholesterol depletion, cells were incubated for 1 h at 37°C in serum-free DMEM containing 0.05 to 0.5% methyl-β-cyclodextrin. To replace cholesterol, the medium was exchanged with serum-free DMEM containing 0.2 mM water-soluble cholesterol, and cells were incubated at 37°C for another hour under continuous mixing. Control cells were incubated in serum-free DMEM without methyl-β-cyclodextrin and water-soluble cholesterol for 2 h. Differences in osmolarity among solutions were compensated with sucrose. Cells were thoroughly washed with ES before electrophysiological experiments.

Cholesterol Assay. Cells were washed twice with 1 ml of ice-cold phosphate-buffered saline, and lipids were extracted with 2 ml of hexane/isopropyl alcohol (3:2, v/v) for 1 h at room temperature. The organic extract was removed, and the solvent was evaporated under a stream of nitrogen. The lipid residue was solubilized in 20 μl of 2-propanol and 10% Triton X-100, and free cholesterol was quantified by spectrophotometry at 562 nm (SpectraMax Plus 384; Molecular Devices, Sunnyvale, CA), according to the manufacturer's instructions (cholesterol/cholesteryl ester quantification kit; Calbiochem, San Diego, CA). After lipid extraction, the residual cell monolayer was solubilized for 15 min at 4°C with 1 ml of radioimmunoprecipitation assay lysis buffer (Santa Cruz Biochemicals, Santa Cruz, CA). The resulting lysate was transferred to a 1.5-ml Eppendorf tube and centrifuged at 10,000*g* for 10 min at 4°C. Protein content was determined in aliquots using the Bradford reagent (Sigma-Aldrich, St. Louis, MO).

Membrane $PI(4,5)P_2$ Depletion. HEKh293Slo cells were triple-transfected with the depletion constructs containing PH-GFP, FRB-CFP, and mRFP-FKBP12–5Pase (active construct) or mRFP-FKBP12 (inactive construct). Cells were incubated with 100 nM rapamycin for at least 3 to 5 min before the experiment to trigger the depletion of $PI(4,5)P_2$ in transfected cells (for details, see Varnai et al., 2006).

Drugs. Rapamycin was purchased from BioSource International (Camarillo, CA). Arachidonic acid, URB597, ARA-S, anandamide, and virodhamine were from Cayman Chemical Co. (Ann Arbor, MI). *N*-Arachidonoyl-D-serine was synthesized as described previously (Milman et al., 2006). 2-AG and 14,15-epoxyeicosa-5(*Z*)-enoic acid (14,15-EEZE) were synthesized by Dr. J. R. Falck. 11,12-EET was from Tocris Bioscience (Ellisville, MO). $PI(4,5)P_2$ was from Calbiochem. O-1918 was synthesized as described previously by Begg et al., (2003). 1-Aminobenzotriazole, 4-amino pyridine, staurosporine, 1-(4-chlorobenzoyl)-5-methoxy-2-methyl-3-indoleacetic acid (indomethacin), nordihydroguaiaretic acid (NDGA), iberiotoxin, NS 1619, pertussis toxin, (*R*)-(−)-1-(3-hydroxyphenyl)-2-methylaminoethanol hydrochloride (phenylephrine), BAPTA, methyl-β-cyclodextrin, water-soluble cholesterol (powder, containing approximately 40 mg of cholesterol balanced with 1 g of methyl-β-cyclodextrin), guanosine 5′-[β-thio]-diphosphate (GDP-β-S), NaGTP, and thapsigargin were from Sigma-Aldrich. For most drugs, stock solutions were prepared in dimethyl sulfoxide, with the exception of NS 1619, indomethacin, NDGA, anandamide, and virodhamine, which were dissolved in ethanol, and 1-aminobenzotriazole, 4-amino pyridine, iberiotoxin, 14,15-EEZE, phenylephrine, $PI(4,5)P_2$, and rapamycin, which were dissolved in water. *N*-Arachidonoyl-L-serine was provided by the manufacturer as an ethanol solution.

Stock solutions were stored under nitrogen and diluted right before the experiment. The concentration of ethanol and dimethyl sulfoxide in the working solution did not exceed 0.05% (v/v). Solutions of methyl-β-cyclodextrin and water-soluble cholesterol were prepared in serum-free DMEM. Cannabinoids were administered in the ES through a multichannel fast perfusion system, having an exchange time in the 100-ms range. Two millimolar GDP-β-S and 100 μM $PI(4,5)P_2$ were infused into the cell in the IS for 5 min before the recording was initiated. Thapsigargin (1 μM), staurosporine (1 μM), 1-aminobenzotriazole (20 μM), NDGA (10 μM), indomethacin (80 μM), URB597 (10 μM), and 14,15-EEZE (20 μM) were added to the ES for 30 min before recording, and pertussis toxin (1 μg/ml) was added to the cell culture medium for 12 h before recording. The exposure times and concentrations of various modulators used in the present study have proven effective in other experimental designs (Jakab et al., 1997; Fukao et al., 2001; Begg et al., 2003; Dubey et al., 2003; Tarzia et al., 2003; Watanabe et al., 2003; Gauthier et al., 2005; Milman et al., 2006). BAPTA was dissolved directly into the intracellular solution.

The online MaxChelator software (http://www.stanford.edu/~cpatton/maxc.html) was used to calculate free $[Ca^{2+}]_i$ in the intracellular solution. Thus, free $[Ca^{2+}]_i$ was adjusted to 100 nM, 250 nM, 500 nM, 1 μM, or 1.5 μM by the administration to the IS of 1.99, 3.32, 5.53, 7.30, or 8.35 mM $CaCl_2$, respectively, in the presence of 0.01 M BAPTA. After each experiment, the superfusion apparatus was thoroughly washed with ethanol and distilled water to avoid any carryover of ligands.

Statistical Analyses. For acquisition and analysis of myograph data, emka TECHNOLOGIES software (emka TECHNOLOGIES France, Paris, France) was used. Relaxant/contractile responses to ARA-S were expressed as a percentage of the phenylephrine/KCl-induced tone.

The effects of ligands on the outward potassium current were expressed in absolute terms or as a ratio of the pretreatment control current amplitudes (I_{ligand}/I_{time0}). A Boltzmann fit using the equation $g = 1/[1 + \exp - (V - V_{1/2})/k]$, where g is conductance, V is membrane potential, $V_{1/2}$ is the activation potential midpoint, and k is the slope, was used to calculate G_{max} and $V_{1/2}$. The potencies of ARA-S and anandamide were expressed as pEC_{50} values ($-\log EC_{50}$[M]) and that of virodhamine and O-1918 as pIC_{50} values ($-\log IC_{50}$[M]) calculated from the Hill equation, $y = 1/[1 + (x - C_{50})^a]$, where y is the response, x is the drug concentration, C_{50} is the concentration of drug producing 50% of the maximal effect, and a is the Hill coefficient.

Channel open probability (NP_o) in cell-attached mode was determined from 2-min recordings by fitting the sum of Gaussian functions to an all-points histogram plot. The NP_o was defined as the time spent in an open state divided by the total time of the analyzed record. When multiple channels occupied a patch, channel activity was calculated as $NP_o = \Sigma n P_n$, where P_n is the probability of finding n channels open.

General statistical data analysis was performed using Prism 4 (GraphPad Software Inc., San Diego, CA). Values are presented as means ± S.E.M. Student's t test for unpaired or paired data were used for comparison of values between two groups as appropriate. For multiple comparisons, one-way analysis of variance followed by Dunnett test was used. Differences were considered significant when $P < 0.05$.

Results

Effect of ARA-S on Rat Mesenteric Artery. As illustrated in Fig. 1, ARA-S relaxed rat isolated mesenteric arteries with intact endothelium precontracted with 5 μM phenylephrine (pEC_{50}, 5.49 ± 0.18; $n = 6$). The response to ARA-S was only slightly, but not significantly, affected by denudation (pEC_{50}, 5.14 ± 0.15; $n = 5$). In both preparations, 100 nM iberiotoxin, a selective BK_{Ca} channel inhibitor (Galvez et al., 1990), produced marked rightward shifts of the ARA-S concentration-response curves (pEC_{50}, 4.76 ± 0.17 in intact and 4.61 ± 0.13 in denuded arteries, $P < 0.05$ compared with respective controls; $n = 5–8$). The increase in tone induced by phenylephrine did not differ between intact and denuded vessels (0.85 ± 0.24 and 1.16 ± 0.23 g, respectively; $n = 5–6$) and was not affected by iberiotoxin (0.98 ± 0.06 and 0.77 ± 0.09 g, respectively; $n = 5–8$). In contrast, ARA-S failed to relax arteries precontracted with 60 mM KCl and caused additional contractions in either intact or endothelium-denuded vessels (pEC_{50}, 5.48 ± 0.16 and 4.82 ± 0.15, respectively; $n = 3$; Fig. 1). The increase in tone produced by KCl was similar between treatment groups (0.53 ± 0.04 and 0.56 ± 0.03; $n = 3–4$).

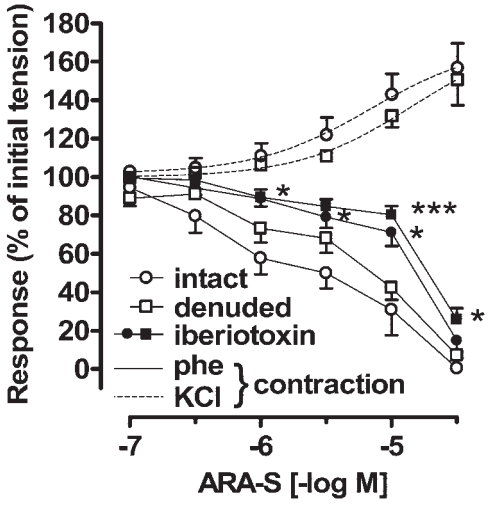

Fig. 1. Effects of ARA-S isolated rat mesenteric arteries. Isolated segments of rat mesenteric arteries were precontracted with 5 μM phenylephrine (phe) or 60 mM KCl. Cumulative concentration-response curves to ARA-S were constructed in intact and denuded arteries under control conditions and in the presence of 100 nM iberiotoxin. Each point represents three to six experiments. *, $P < 0.05$; ***, $P < 0.001$ compared with arteries not treated with iberiotoxin.

Characterization of Whole-Cell Outward Currents in HEK293hSlo Cells. Native HEK293 cells do not endogenously express BK_{Ca} channels. Thus, the effects of endocannabinoids were studied in HEK293hSlo, as confirmed by RT-PCR (Fig. 2a).

In HEK293hSlo cells held at −60 mV, a series of voltage steps produced a noninactivating, voltage-dependent, whole-cell outward current, which was absent in native HEK293 cells. This current was completely blocked by 100 nM iberiotoxin (Fig. 2b) but was not affected by 5 μM 4-amino pyridine, an inhibitor of voltage-gated potassium channels (Jiang et al., 2002); after the 90-mV step, the current was 93.2 ± 9.3% of control in the presence of 4-amino pyridine ($n = 6$). Analysis of the tail currents revealed a reversal potential of −87.6 ± 2.5 mV ($n = 6$; data not shown), similar to the predicted value for K^+ using the Nernst equation being −97.5 mV. This indicates that K^+ is the predominant ion carrying the outward current.

The magnitude of the whole-cell outward K^+ current and the relative voltage-conductance relationship curves varied with the concentration of free $[Ca^{2+}]_i$. Thus, the $V_{1/2}$ values were 117.2 ± 2.6, 93.6 ± 1.5, 67.3 ± 1.6, and 43.3 ± 1.9 mV ($n = 6$; $P < 0.05$), when free $[Ca^{2+}]_i$ was clamped at 0.1, 0.5, 1.0, and 1.5 μM, respectively, with corresponding k values of 21.55 ± 3.14, 21.71 ± 1.92, 16.65 ± 1.78, and 16.82 ± 2.90, respectively (data not shown). In most experiments, free $[Ca^{2+}]_i$ was fixed at 1 μM.

The peak whole-cell outward K^+ current at +60 mV (I_{max}) was similar among cells tested on the same day but varied from 389.9 ± 49.3 to 861.5 ± 62.2 pA/pF ($n = 4–6$; $P < 0.001$) on a day-to-day basis. To test the effect of endocannabinoids and related ligands, a voltage step that represented 20% of I_{max} was applied to cells. This voltage ranged from 86.5 ± 0.8 to 94.0 ± 2.5 mV ($n = 5–6$) in different batches of cells. For consistency, the expression "~90-mV step" will be used throughout the article to cover the above range, whereas "90-mV step" will be used when experiments were performed exactly at this step.

Effects of ARA-S on the Whole-Cell Outward K^+ Current in HEK293hSlo Cells. Application of 3 μM ARA-S markedly enhanced the whole-cell outward K^+ current, and it was still nearly completely blocked by 100 nM iberiotoxin. The effect of ARA-S reached a maximum within 15 to 30 s and was rapidly reversed upon removal of the drug (Fig. 2c). In the presence of the selective BK_{Ca} channel opener NS 1619, ARA-S further increased this current, and it remained sensitive to iberiotoxin (Fig. 2c).

As shown in Fig. 2d, ARA-S enantiomers increased BK_{Ca}

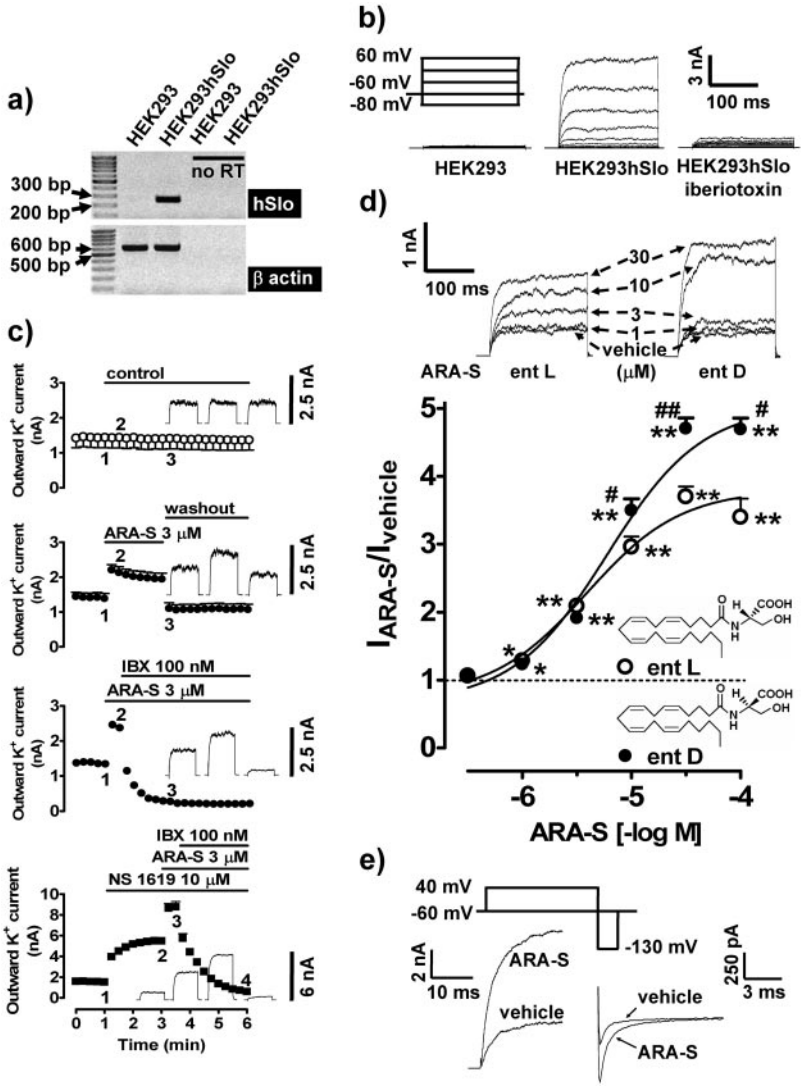

Fig. 2. Effect of ARA-S on the whole-cell outward current in HEK293hSlo cells. a, RT-PCR documenting human BK_{Ca} channel α-subunit (hSlo) mRNA in stably transfected HEK293hSlo cells. β-Actin was used as the control (no RT, no reverse transcription). b, outward current traces from native (HEK293) and stably transfected (HEK293hSlo) cells obtained by the voltage step protocol. Iberiotoxin (100 nM) was present in the medium for 2 min before the experiment. c, time-dependent effect of vehicle (control), ARA-S, NS 1619, and iberiotoxin (IBX) on the outward K^+ current. The current was generated by the ~90-mV step from a holding potential of −60 mV. Bars, vehicle/drug application periods. Original traces correspond to the 200-ms currents recordings obtained at indicated time points. $n = 3$. Error bars are enclosed within symbols at various time points. d, concentration-dependent effect of ARA-S enantiomers (ent; chemical structures included in the figure) on the whole-cell outward K^+ current generated by the ~90-mV step. Cells were exposed to ARA-S enantiomers for 15 s. The current amplitude in cells treated with the vehicle was taken as unity (dashed line). $n = 4$–7; *, $P < 0.05$; **, $P < 0.01$ compared with the vehicle-treated cells; #, $P < 0.05$, ##, $P < 0.01$ compared with the ARA-S L-enantiomer. Original traces correspond to the current stimulated by the ~90-mV step. e, sample traces of the outward potassium current during the depolarization step (left) and repolarization step (right) produced by tail current protocol in the presence of 10 μM ARA-S or its vehicle.

channel activity in a concentration-dependent fashion. The respective pEC_{50} values for the L- and D-enantiomers were not different, i.e., 5.63 ± 0.21 versus 5.32 ± 0.13 ($n = 5$–6). The maximal response was significantly higher for the D-relative to the L-enantiomer (Fig. 2d). Because *N*-arachidonoyl L-serine was earlier described as an endogenous lipid in the porcine brain (Milman et al., 2006), the effects of this enantiomer will be described in the remainder of this study.

Application of ARA-S caused a concentration-dependent leftward shift of the relative voltage-conductance relationship curves. The $V_{1/2}$ values were 58.6 ± 2.0, 49.3 ± 1.5, and 40.0 ± 1.8 mV in cells exposed to vehicle and 3 and 10 μM ARA-S, respectively ($n = 6$; $P < 0.001$). The corresponding k values were 18.4 ± 2.7, 17.5 ± 2.3, and 15.9 ± 2.4 (data not shown).

In control cells, activation time constants measured from single exponential fits to the 100-mV depolarization step averaged 4.3 ± 0.5 ms ($n = 7$) and remained unchanged after exposure to 3 and 10 μM ARA-S (3.9 ± 0.2 and 3.7 ± 0.1 ms, respectively; $n = 6$–7; Fig. 2e). The current deactivation time constant was quantified by single exponential fits to the decaying phase of the tail current by a step from +40 to −130 mV. In control cells, the decay time constant was 0.19 ± 0.01 ms ($n = 7$) and was also unaffected in the presence of either ARA-S concentrations (0.17 ± 0.01 and 0.21 ± 0.01 ms, respectively; $n = 6$–7; Fig. 2e).

The current density generated by the 90-mV depolarization step from the holding potential did not significantly differ between cells infused via the patch pipette with 10 μM ARA-S (269.3 ± 56.6 pA/pF; $n = 6$) or its vehicle (174.7 ± 27.0 pA/pF; $n = 6$). The presence of 10 μM ARA-S inside the cell did not alter the magnitude of the response to 3 μM ARA-S applied on the extracellular cell surface (respective $I_{ARA\text{-}S}/I_{time0}$ values were 1.44 ± 0.04 and 1.51 ± 0.04 in cells pretreated with 10 μM ARA-S or vehicle via patch pipette; $n = 6$).

Effects of ARA-S on the Outward K^+ Current in HEK293hSlo Cells Cotransfected with the β_1 Subunit. The presence of the β_1 subunit in HEK293hSlo cells (HEK293hSloβ_1) produced a leftward shift in the relative voltage-conductance relationship curve (Fig. 3a), decreasing the respective $V_{1/2}$ values from 47.2 ± 3.1 to 34.8 ± 1.9 mV ($P < 0.001$; $n = 5$–6; the k values under the same conditions were 16.2 ± 2.5 and 15.9 ± 1.6). As a consequence, the voltage step was also adjusted from 89.8 ± 1.1 to 76.2 ± 1.7 mV to produce a K^+ current of 2.28 ± 0.08 and 2.34 ± 0.05

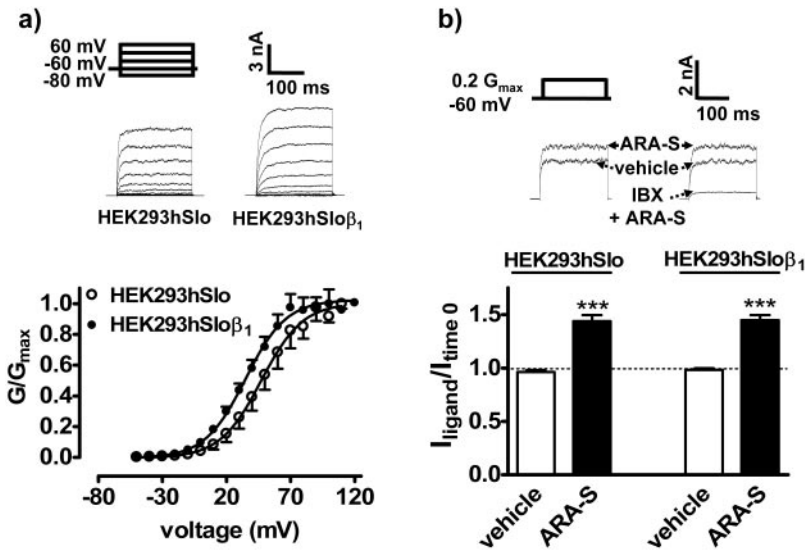

Fig. 3. Effect of ARA-S on the whole-cell outward current in HEK293hSlo cells cotransfected with β_1 subunit. a, relative conductance (G/G_{max})-voltage relationship curves and sample traces in mock-transfected cells (HEK293hSlo) or in cells cotransfected with the human β_1 subunit (HEK293hSloβ_1). The outward potassium current was generated by the series of voltage steps from the holding potential of −60 mV. n = 5–6. b, effect of ARA-S on the whole-cell outward K^+ current in mock-transfected cells (HEK293hSlo) or in cells cotransfected with the human β_1 subunit (HEK293hSloβ_1). The current was generated by a single voltage step of 89.8 ± 1.1 (HEK293hSlo) and 75.2 ± 1.7 mV (HEK293hSloβ_1), corresponding to 0.2 G_{max}. Each point represents five to six experiments. Original recordings are representative of the figure. Iberiotoxin (IBX; 100 nM) was present for 2 min before the application of 3 μM ARA-S or vehicle.

nA, respectively (n = 5–6), corresponding to 0.2 G_{max}. As shown in Fig. 3b, the response to ARA-S was not altered by the β_1 subunit. The amplitude of the K^+ current in HEK293hSloβ_1 cells after ARA-S application was sensitive to 100 nM iberiotoxin (inhibition by 85.0 ± 3.7%; $P < 0.001$; n = 3; see also Fig. 3b).

Effects of ARA-S on the Outward K^+ Current in Whole Cells, Cell-Attached Mode, and Outside-out Patches Obtained from HEK293hSlo Cells. A series of voltage steps produced a noninactivating voltage-dependent macroscopic outward K^+ current in excised outside-out patches, which was of much smaller amplitude than that observed in whole-cell recordings, but had similar $V_{1/2}$ value of the relative conductance-voltage relationship curves (72.5 ± 1.3 and 71.9 ± 3.2 mV, respectively; n = 3–5; Fig. 4a). The corresponding k values for the recording at different configurations were 14.9 ± 5.5 and 17.5 ± 1.6. As shown in Fig. 4b, the sensitivity of excised patches to ARA-S was reduced relative to whole cells ($P < 0.01$ for ratios $I_{ARA\text{-}S}/I_{vehicle}$ at every time point). Thus, the excised patches were not sensitive to 3 μM ARA-S and produced maximally 42.1 ± 4.0% (n = 6) of the potentiation observed in whole cells when exposed to 10 μM ARA-S. In contrast, 10 μM NS 1619 was equally effective in the two recording configurations (Fig. 4b).

Application of ARA-S in cell-attached mode followed the same pattern as in isolated patches (Fig. 4c). The NP_o in cells before treatment was 0.035 ± 0.007 (n = 12). This value was not significantly altered by 3 μM ARA-S but increased 2-fold by 10 μM ARA-S by increasing the frequency of channel openings (from 159.78 ± 30.28 to 204.46 ± 31.10 Hz, $P < 0.05$; n = 4) and time spent in an open state (peak half width; from 0.75 ± 0.04 to 0.83 ± 0.05 ms; $P < 0.05$; n = 4). The response was sensitive to iberiotoxin (Fig. 4c). The current amplitude did not differ among cells treated for 2 min with vehicle and 3 to 10 μM ARA-S (9.20 ± 0.17, 9.23 ± 0.11, and 9.31 ± 0.09, respectively; n = 4).

G Proteins, Cytosolic Factors, and Free $[Ca^{2+}]_i$ Are Not Involved in the Effects of ARA-S. The potentiation of the whole-cell K^+ current by ARA-S was not affected by the irreversible G protein inhibitor GDP-β-S, specific $G_{i/o}$ protein inhibitor pertussis toxin, or by the broad-spectrum protein kinase inhibitor staurosporine (Table 1). Likewise, the epoxyeicosatrienoic acid antagonist 14,15-EEZE, cyclooxygenase inhibitor indomethacin, lipoxygenase inhibitor NDGA, fatty acid amide hydrolase inhibitor URB597, and cytochrome P-450 inhibitor 1-aminobenzotriazole were without effect on the response of HEK293hSlo cells to ARA-S (Table 1).

Clamping free $[Ca^{2+}]_i$ at 100 nM, 500 nM, 1 μM, and 1.5 μM required different absolute voltages (140.8 ± 2.2, 120.0 ± 2.1, 105.7 ± 2.1, and 88.8 ± 1.9 mV, respectively; n = 4–6) to produce whole-cell outward K^+ current (1.9 ± 0.1, 2.5 ± 0.1, 2.4 ± 0.2, and 2.2 ± 0.1 nA) equivalent to 0.2 G_{max}. With the exception of the lowest $[Ca^{2+}]_i$, application of 3 μM ARA-S caused a similar potentiation of K^+ current at all other $[Ca^{2+}]_i$ concentrations (the respective $I_{ARA\text{-}S}/I_{time0}$ values were 1.96 ± 0.04, 1.71 ± 0.06, 1.68 ± 0.04, and 1.66 ± 0.02; n = 4–6; $P < 0.01$, according to one-way analysis of variance). In addition, pretreatment of HEK293hSlo cells for 30 min with the sarcoplasmic reticulum ATPase inhibitor 1 μM thapsigargin did not affect the whole-cell outward K^+ currents induced by the 90-mV depolarization step (2.1 ± 0.4 nA with vehicle and 2.0 ± 0.3 nA with thapsigargin; n = 4–5) or its potentiation by 3 μM ARA-S (the respective $I_{ARA\text{-}S}/I_{time0}$ values were 1.71 ± 0.06 and 1.69 ± 0.07 in vehicle- and thapsigargin-pretreated cells; data not shown).

The Effect of Cholesterol Depletion/Repletion on the ARA-S Response. Incubation of HEK293hSlo cells with the cholesterol depleting agent methyl-β-cyclodextrin did not affect the current-voltage relationship curves. The basal current generated by the ~90-mV step from holding potential was 2.17 ± 0.21 nA in the control group (n = 9) and 2.46 ± 0.13, 2.34 ± 0.23, 2.54 ± 0.27, and 1.93 ± 0.24 nA in cells treated with increasing concentrations of methyl-β-cyclodextrin (n = 3–9; see original recording, Fig. 5). Methyl-β-cyclodextrin inhibited the ARA-S enhancement of whole-cell outward K^+ currents in a concentration-dependent manner (Fig. 5). Complete inhibition of the ARA-S effect occurred at 0.5% (3.8 mM) methyl-β-cyclodextrin. In contrast, 0.5% methyl-β-cyclodextrin did not affect the response to 10 μM NS 1619 (the I_{120s}/I_{time0} values were 3.37 ± 0.24 and 3.26 ± 0.22 in the control and methyl-β-cyclodextrin pretreated cells, respectively; n = 5). As shown earlier (Sarker and Maruyama, 2003), methyl-β-cyclodextrin at concentrations up to 5 mM

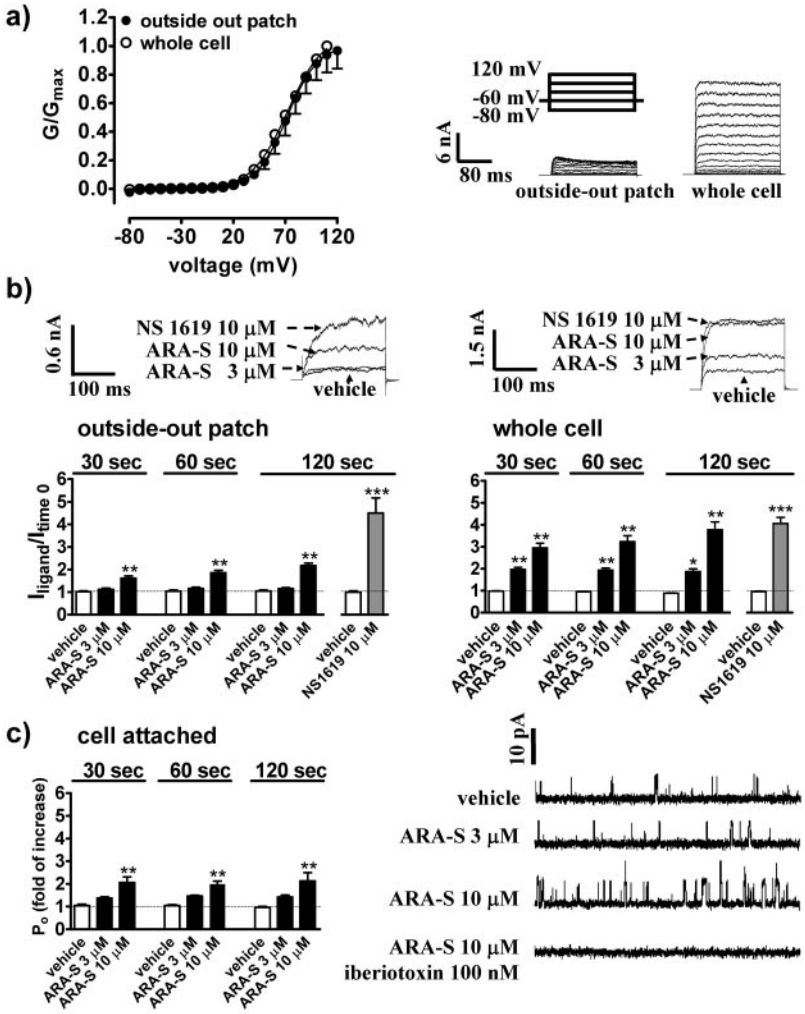

Fig. 4. Comparison of ARA-S effects in various electrophysiological recording modes in HEK293hSlo cells. a, relative conductance (G/G_{max})-voltage relationship curves and sample traces of outward K^+ current in whole cells and isolated patches produced by the voltage step protocol. Each point represents three to five experiments. b, influence of ARA-S, NS 1619, and vehicle on the outward K^+ current in isolated outside-out patches and in whole cells. The current was generated by the ~90-mV step from a holding potential of −60 mV before (time 0) and after application of ligand or its vehicle. n = 3–6. c, effect of ARA-S on the BK_{Ca} channel activity in cell-attached mode. Cells were voltage clamped at a holding potential of +40 mV. ARA-S or its vehicle was applied on the cell surface. Iberiotoxin was present in the pipette for 2 min. Each point represents four experiments. Traces are representative of 250-ms recording obtained 2 min after ARA-S application. *, $P < 0.05$; **, $P < 0.01$ compared with cells treated with the vehicle.

TABLE 1

Influence of various inhibitors on the effect of *N*-arachidonoyl L -serine in HEK293 hSlo cells

Cells were incubated with solvents (control) or with 14,15-EEZE, staurosporine, indomethacin, NDGA, URB597, 1-aminobenzotriazole (for 30 min), or pertussis toxin (12 h) or were infused with GDP-β-S for 5 min before experiment. The current was generated before (I_{time0}) and 30 s after the application of 3 μM ARA-S or vehicle (I_{ligand}) by a voltage step of 98.3 ± 0.88 mV (control for GDP-β-S) and 114.5 ± 1.71 mV (GDP-β-S), corresponding to 0.2 G_{max} or by ~90 mV (other treatment groups). Results are presented as means ± S.E.M. (n = number of experiments).

Treatment	I_{time0}	I_{ligand}/I_{time0}		n
		Vehicle	ARA-S	
	nA			
Control	2.34 ± 0.13	1.00 ± 0.01	1.57 ± 0.02*	6
GDP-β-S, 2 mM	2.27 ± 0.13	0.98 ± 0.03	1.55 ± 0.04*	6
Control	1.71 ± 0.09	1.00 ± 0.01	1.51 ± 0.03*	8
Pertussis toxin, 1 μg/ml	1.87 ± 0.18	1.00 ± 0.01	1.49 ± 0.02*	12
Control	1.49 ± 0.09	1.02 ± 0.02	1.59 ± 0.07*	5
14,15-EEZE, 20 μM	1.60 ± 0.07	1.01 ± 0.01	1.43 ± 0.05*	5
Control	1.81 ± 0.17	0.96 ± 0.06	1.68 ± 0.03*	6
Staurosporine, 1 μM	1.84 ± 0.15	0.99 ± 0.11	1.65 ± 0.05*	6
Control	1.67 ± 0.20	0.93 ± 0.05	1.80 ± 0.02*	3
Indomethacin, 10 μM	1.70 ± 0.63	0.94 ± 0.01	1.81 ± 0.01*	3
Control	1.48 ± 0.12	0.97 ± 0.01	1.73 ± 0.03*	4
NDGA, 10 μM	1.62 ± 0.11	0.97 ± 0.01	1.82 ± 0.01*	3
Control	1.59 ± 0.11	0.97 ± 0.03	1.73 ± 0.02*	3
URB597, 10 μM	1.64 ± 1.36	0.96 ± 0.06	1.57 ± 0.07*	3
Control	2.07 ± 0.11	0.97 ± 0.08	1.73 ± 0.03*	4
1-Aminobenzotriazole, 20 μM	2.09 ± 0.21	1.00 ± 0.10	1.63 ± 0.05*	5

* $P < 0.001$ compared with vehicle.

had no toxic effect on the cell. Repletion of cholesterol to previously depleted membranes by exposure to 0.2 mM water-soluble cholesterol restored the response to ARA-S (Fig. 5). Changes in the current potentiation by ARA-S after cholesterol depletion and reconstitution correlated with the changes in cellular cholesterol content (Table 2).

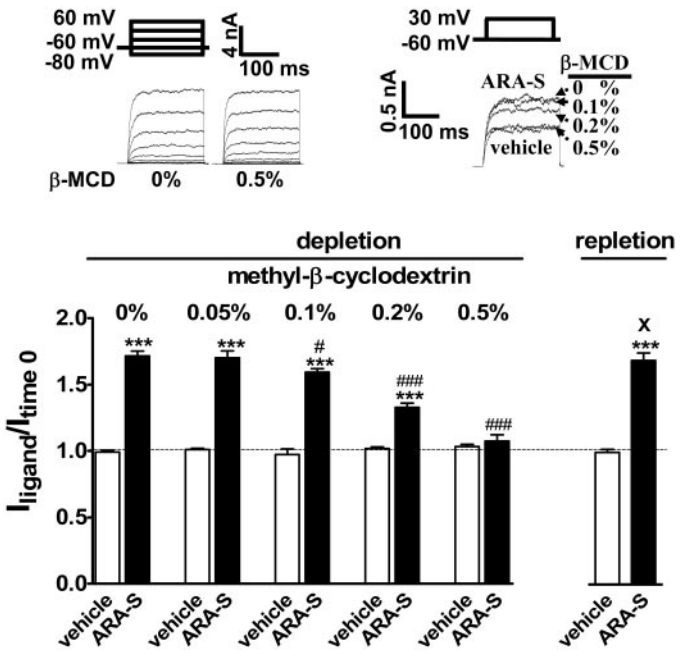

Fig. 5. Influence of cholesterol manipulation on the effect of ARA-S in HEK293hSlo cell. Cells were preincubated with indicated concentrations of methyl-β-cyclodextrin (β-MCD; depletion) followed by 0.2 mM water-soluble cholesterol (repletion). Control cells were treated with DMEM (for details, see *Materials and Methods*). The current was generated by a single ~90-mV step before (I_{time0}) and after application of 3 μM ARA-S or its vehicle (I_{ligand}). The current amplitude before treatment was taken as unity (dashed line). Each bar represents three to nine experiments. ***, $P < 0.001$ compared with the vehicle-treated cells. #, $P < 0.05$; and ###, $P < 0.001$ compared with cells not incubated with methyl-β-cyclodextrin. X, $P < 0.001$ compared with cells treated with 0.5% methyl-β-cyclodextrin. The original recordings represent outward currents obtained from cells treated by the voltage step protocol (left) or are representative of the figure (right).

TABLE 2

Cholesterol content in HEK293 hSlo cells

Cells were incubated for 1 h with 0.5% methyl-β-cyclodextrin (depletion) followed by incubation with 0.2 mM water-soluble cholesterol (repletion). Control cells were incubated in serum-free DMEM. Lipids were then extracted for cholesterol quantification. Results are presented as means± S.E.M. (n = number of experiments).

Treatment	Cholesterol Content	n
	μg/mg protein	
Control	34.67 ± 0.47	6
Depletion	25.25 ± 0.44*	6
Repletion	40.50 ± 0.94*#	6

* $P < 0.01$ compared with control.
# $P < 0.001$ compared with cells undergoing cholesterol depletion.

Membrane $PI(4,5)P_2$ Alters the Whole-Cell K^+ Current in HEK293hSlo Cells but Does Not Affect the Response to ARA-S. As shown earlier (Varnai et al., 2006), rapamycin at the concentration of 100 nM triggers an immediate depletion of $PI(4,5)P_2$ in transfected cells. In the present study, rapamycin treatment caused a small but significant rightward shift of the relative voltage-conductance relationship curve in HEK293hSlo cells transfected with the active $PI(4,5)P_2$-depletion construct. The $V_{1/2}$ values were 49 ± 1.9 and 56.9 ± 1.1 mV ($P < 0.001$; n = 5–6), and the corresponding k values were 17.2 ± 1.6 and 19.1 ± 0.8 in cells transfected with the inactive (control) and active depletion constructs, respectively. The magnitude of the response to 3 μM ARA-S did not differ between constructs ($I_{ARA\text{-}S}/I_{time0}$ values were 1.54 ± 0.04 and 1.46 ± 0.05, respectively; n = 5–6; data not shown).

Infusion of 100 μM $PI(4,5)P_2$ into the cell only tended to shift the relative voltage-conductance relationship curve to the left. The $V_{1/2}$ values were 82.7 ± 1.5 and 78.8 ± 1.1 mV (n = 6), and the corresponding k values were 14.7 ± 1.2 and 18.7 ± 1.8 in cells treated with vehicle and $PI(4,5)P_2$, respectively. Infusion of $PI(4,5)P_2$ to the cell did not alter the response to 3 μM ARA-S ($I_{ARA\text{-}S}/I_{time0}$ ratios were 1.59 ± 0.03 and 1.51 ± 0.04, respectively; n = 6; data not shown).

Effect of Ligands Structurally Related to ARA-S on the Whole-Cell Outward K^+ Current in HEK293hSlo Cells. Anandamide increased the whole-cell outward K^+ current in a concentration-dependent fashion (pEC_{50} of 5.32 ± 0.24; n = 4–6; Fig. 6a). The efficacy of the response to anandamide was significantly lower than for ARA-S ($I_{ligand}/I_{control}$ ratio was 2.31 ± 0.32 and 2.31 ± 0.15, respectively; $P < 0.01$; n = 4–6; for comparison, see also Figs. 2d and 6a). In contrast, arachidonic acid was less potent than ARA-S (pEC_{50} was 4.78 ± 0.19; $P < 0.05$; n = 3; Fig. 6a) but had similar maximal effect ($I_{ligand}/I_{control}$ ratio was 3.54 ± 0.38; for comparison, see also Figs. 2d and 6a). 2-AG and the epoxylated derivative of arachidonic acid, 11,12-EET, were inactive in the present study up to 10 μM (Fig. 6a). Incubation of cells with virodhamine inhibited the whole-cell outward K^+ current in HEK293hSlo cells (pIC_{50} value of 6.35 ± 0.16; n = 3–5; Fig. 6b). The inhibitory effect also occurred in outside-out patches exposed to 10 μM virodhamine (inhibition by 60.0 ± 7.0%, $P < 0.05$ compared with control; n = 8; data not shown).

Effects of O-1918 on Outward K^+ Current. The synthetic cannabinoid analog O-1918 inhibited the whole-cell

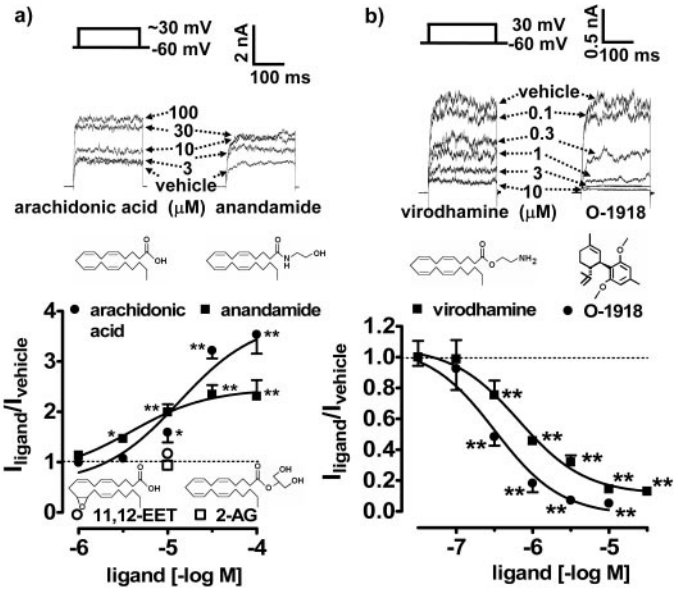

Fig. 6. Effect of O-1918 and ligands structurally related to ARA-S on the whole-cell outward current in HEK293hSlo cells. Cells were exposed to: a, anandamide, arachidonic acid (for 2 min), 11,12-EET, and 2-arachidonoyl glycerol (for 5 min); and b, virodhamine, O-1918 (for 10 min; chemical structures included in the figure), or their vehicles. The current was generated by the ~90-mV step (*a*) or by the 90-mV step (*b*) from a holding potential of −60 mV. The current amplitude in cells treated with the vehicle was taken as unity (dashed line). n = 3–7. Error bars are enclosed within symbols at high concentrations of inhibitory ligands. *, $P < 0.05$; **, $P < 0.01$ compared with the vehicle-treated cells. Original traces are representative of the figure.

outward K^+ current in HEK293hSlo cells with a pIC_{50} value of 6.59 ± 0.16 (n = 3–6; Fig. 6b). The inhibitory effect of O-1918 was also reflected by the rightward shift of the $V_{1/2}$ values of the relative conductance-voltage curve (from 59.6 ± 1.4 mV in the presence of vehicle to 65.5 ± 3.6, 82.0 ± 1.2, 92.9 ± 2.6, 127.5 ± 5.7, and 132.8 ± 8.2 mV in the presence of 0.1–10 μM O-1918) and no changes in k values. The whole-cell outward potassium current of 2.26 ± 0.06 (n = 12), corresponding to 0.2 G_{max}, was generated in the presence of 1 μM O-1918 or its vehicle as a control by a voltage step of 121.5 ± 2.6 (n = 6) and 92.7 ± 1.2 (n = 6) mV, respectively. Application of 3 μM ARA-S increased this current by 90.7 ± 4.9% (n = 6) in control cells and by 55.1 ± 1.9% (n = 6) in the presence of 1 μM O-1918 (inhibition by approximately 40%; $P < 0.001$ compared with the control). O-1918 (1 μM) also effectively inhibited the current in outside-out patches stimulated by the 90-mV step (inhibition by 85.4 ± 1.5%; $P < 0.001$; n = 3; data not shown).

Discussion

The present findings provide evidence that the recently identified endogenous lipoamine ARA-S is an activator of BK_{Ca} channels, which accounts for its vasodilator action. In phenylephrine-preconstricted rat mesenteric arteries, ARA-S produced largely endothelium-independent vasorelaxation, which was inhibited by iberiotoxin, implicating the involvement of vascular BK_{Ca} channels. Moreover, ARA-S caused vasoconstriction when vessels were preconstricted with KCl, which further supports its vasorelaxant effect through K^+ channels. In some preparations, ARA-S has been shown previously to have endothelium-dependent and -independent vasorelaxant components, both sensitive to O-1918 (Milman et al., 2006), suggesting that this synthetic cannabinoid may also target smooth muscle channels. Indeed, as discussed below, O-1918 is a potent inhibitor of BK_{Ca}-gated K^+ currents.

CB_1 receptors mediate vasorelaxation in some vessels by increasing the activity of BK_{Ca} channels (Romano and Lograno, 2006). However, ARA-S does not bind to CB_1 receptors, and its effect is resistant to pertussis toxin (Milman et al., 2006), which resembles the BK_{Ca} channel-dependent, CB_1/CB_2 receptor-independent vasorelaxation by anandamide in rat mesenteric (Plane et al., 1997; Járai et al., 1999) and coronary (White et al., 2001) arteries.

Additional evidence for BK_{Ca} channels being a direct molecular target of ARA-S is the ability of ARA-S to potentiate BK_{Ca} currents in HEK293hSlo cells. The presence of the functional BK_{Ca} channel α subunit in HEK293hSlo cells was confirmed by RT-PCR and by the sensitivity of the outward current to voltage, $[Ca^{2+}]_i$, the selective BK_{Ca} channel opener NS 1619 (Olesen et al., 1994), and the BK_{Ca} inhibitor iberiotoxin (Galvez et al., 1990). Although native voltage-gated K^+ channels are present in HEK293 cells (Jiang et al., 2002), the peak current amplitude was not modified by 4-amino pyridine, ruling out their contribution to the total current. To mimic smooth muscle type BK_{Ca} channels, HEK293hSlo cells were cotransfected with the human BK_{Ca} β_1 subunit, which resulted in the expected increase in voltage sensitivity (Brenner et al., 2000). Because potentiation of the BK_{Ca} current by ARA-S was similar in the absence of presence of the β subunit, the α subunit itself is its most likely target.

Similar effects of L- and D-enantiomers of ARA-S indicate the lack of stereoselectivity, which discounts the involvement of specific receptor. As an alternative, an indirect action via membrane lipids is suggested by the loss of ARA-S response after membrane cholesterol depletion and its restoration after cholesterol replenishment. The external membrane event is substantiated by the fact that intracellular application of ARA-S inside the patch pipette did not significantly alter BK_{Ca} channel activity and did modify the effect of ARA-S applied on the extracellular cell surface.

Mechanism of Channel Potentiation by ARA-S. ARA-S potentiated the BK_{Ca} current only when it was applied extracellularly in the whole-cell mode by shifting the voltage-conductance relationship toward more negative potentials. The activation and deactivation time constants were unaffected, suggesting that ARA-S does not directly interact with the gating mechanism of the channel pore. The response to 3 μM ARA-S is reduced in excised patches relative to the whole-cell configuration. This decrease cannot be because of changes in basic channel properties because the BK_{Ca} conductance and the response to NS 1619 remained unchanged. A similar weaker effect was observed when ARA-S was applied to the cell surface in cell-attached mode, suggesting that the compound acts locally. ARA-S augmented the BK_{Ca} current by increasing the channel open probability, similar to the mechanism proposed for the BK_{Ca} channel opener NS 1619 (Olesen et al., 1994; Khan et al., 1998). However, NS 1619 did not modify the effect of ARA-S, suggesting that the two compounds interact with distinct sites on the channel.

The cellular metabolism of ARA-S has not yet been explored. We have considered ARA-S to be a putative substrate for fatty acid amide hydrolase, cyclooxygenase, lipoxygenase, and cytochrome P-450, by analogy to anandamide (Watanabe et al., 2003), arachidonic acid (Fukao et al., 2001), and other fatty acids (Duerson et al., 1996). In particular, cytochrome P450 epoxygenase-derived eicosanoids have been shown to increase BK_{Ca} channel activity in HEK293 cells (Fukao et al., 2001) and produce BK_{Ca} channel-dependent vasorelaxation through specific mechanisms (Gauthier et al., 2005). However, application of potent inhibitors failed to modify ARA-S potentiation of the BK_{Ca} channel, suggesting that its effect is because of the parent compound rather than a metabolite.

Potentiation of BK_{Ca} currents by ARA-S does not involve G protein activation because it remained unaffected by the specific $G_{i/o}$ protein inhibitor pertussis toxin or by GDP-β-S, a nonequilibrium inhibitor of all G proteins. The lack of effect of the broad-range kinase inhibitor, staurosporine, argues against the involvement of kinase-dependent downstream signaling molecules, e.g., mitogen-activated protein kinase, protein kinase B, and cAMP- and cGMP-dependent protein kinases, which are known to modulate BK_{Ca} currents in certain systems (Zhou et al., 2001; O'Malley and Harvey, 2004; Liu et al., 2006) and in endothelial cells (Milman et al., 2006).

The effect of ARA-S in HEK293hSlo cells was largely independent of changes in $[Ca^{2+}]_i$. Only when $[Ca^{2+}]_i$ was clamped at 100 nM was a more pronounced response to ARA-S observed. This may indicate that cellular sensitivity to ARA-S is higher at resting $[Ca^{2+}]_i$ levels and might explain the reported higher potency of anandamide (Sade et al., 2006) relative to that which we observed here in the presence of 1 μM free $[Ca^{2+}]_i$. A reported functional association of

BK_{Ca} channels with sarcoplasmic reticulum (Weaver et al., 2007) could also not account for the effect of ARA-S because it was not modified by the sarcoplasmic reticulum ATPase inhibitor thapsigargin.

Endocannabinoids approach their site of action by interacting with the lipid bilayer and laterally diffusing within the membrane leaflet to the target protein (Makriyannis et al., 2005). To test whether membrane components play a role in the action of ARA-S, we experimentally altered membrane cholesterol levels. Reduction of membrane cholesterol by treatment with methyl-β-cyclodextrin resulted in a loss of response to ARA-S, which could be restored by cholesterol reconstitution. Methyl-β-cyclodextrin treatment did not change the current-voltage relationship or the response to NS 1619, arguing against altered channel properties as the underlying mechanism. The loss of some cytosolic factors during cholesterol depletion is also unlikely because the reconstitution of pure cholesterol into the membrane completely restored the sensitivity of BK_{Ca} channels to ARA-S. Therefore, it is plausible that the state of the plasma membrane plays a crucial role in the ARA-S effect, most likely by allowing the lipophilic arachidonoyl side chain to anchor to the lipid membrane and to access the channel protein. Alternatively, ARA-S may alter cell membrane properties and thus secondarily affect BK_{Ca} channel function. As shown by O'Connell et al. (2006), channel electrophysiological properties are affected by lipid bilayer composition.

The loss of the ARA-S effect in cholesterol-depleted cells parallels the rundown of the ARA-S response after patch excision. It is possible that some membrane lipid factors may be disturbed during patch excision. The membrane phospholipid $PI(4,5)P_2$ is a known regulator of ion channel function (Oliver et al., 2004; Lukacs et al., 2007), but it is not involved in the effect of ARA-S on BK_{Ca} currents, which remained unaffected by depleting or adding $PI(4,5)P_2$ to the preparation.

To explore the structural requirements of BK_{Ca} activation by ARA-S, the effect of ligands structurally related to ARA-S were analyzed in the present study. Thus, arachidonic acid was 10 times less potent than ARA-S, whereas 11,12-EET was inactive. Anandamide was equipotent with ARA-S, but its efficacy was much lower. The presence of an ethanolamine moiety in anandamide seems to be critical because its replacement with glycerol (2-arachidonoyl glycerol) resulted in the loss of effect. Interestingly, virodhamine potently inhibited the BK_{Ca} current, and its inhibitory effect persisted in isolated patches. The nature of channel modulation by above ligands and particularly whether they share a similar mechanism to that of ARA-S still requires further investigation.

The present data indicate that the endothelium-independent component of ARA-S-induced vasodilation is because of the activation of BK_{Ca} channels and that O-1918 is an inhibitor of BK_{Ca}-gated K^+ currents. A similar direct interaction may also account for the activation by ARA-S of N-type Ca^{2+} channels (Guo et al., 2008). Our findings do not negate the possibility that the endothelium-dependent, pertussis toxin-sensitive component of the effect of ARA-S and anandamide, as reported in numerous earlier studies (Járai et al., 1999; Mukhopadhyay et al., 2002; Randall et al., 2004; Milman et al., 2006), may be mediated by an as yet unidentified G protein-coupled receptor.

Acknowledgments

We thank Dr. J. R. Falck for providing 14,15-EEZE used in the study, Dr. Steven Treistman for HEK293hSlo cells and plasmid construct containing the human β_1 subunit, and Dr. Tamas Balla for fusion constructs used for membrane $PI(4,5)P_2$ depletion.

References

Bátkai S, Pacher P, Osei-Hyiaman D, Radaeva S, Liu J, Harvey-White J, Offertáler L, Mackie K, Rudd MA, Bukoski RD, et al. (2004) Endocannabinoids acting at cannabinoid-1 receptors regulate cardiovascular function in hypertension. *Circulation* **110:**1996–2002.

Begg M, Mo FM, Offertaler L, Bátkai S, Pacher P, Razdan RK, Lovinger DM, and Kunos G (2003) G protein-coupled endothelial receptor for atypical cannabinoid ligands modulates a Ca^{2+}-dependent K^+ current. *J Biol Chem* **278:**46188–46194.

Brenner R, Peréz GJ, Bonev AD, Eckman DM, Kosek JC, Wiler SW, Patterson AJ, Nelson MT, and Aldrich RW (2000) Vasoregulation by the beta1 subunit of the calcium-activated potassium channel. *Nature* **407:**870–876.

Dubey RK, Gillespie DG, Zacharia LC, Barchiesi F, Imthurn B, and Jackson EK (2003) CYP450- and COMT-derived estradiol metabolites inhibit activity of human coronary artery SMCs. *Hypertension* **41:**807–813.

Duerson K, White RE, Jiang F, Schonbrunn A, and Armstrong DL (1996) Somatostatin stimulates BKCa channels in rat pituitary tumor cells through lipoxygenase metabolites of arachidonic acid. *Neuropharmacology* **35:**949–961.

Fukao M, Mason HS, Kenyon JL, Horowitz B, and Keef KD (2001) Regulation of BK(Ca) channels expressed in human embryonic kidney 293 cells by epoxyeicosatrienoic acid. *Mol Pharmacol* **59:**16–23.

Galvez A, Gimenez-Gallego G, Reuben JP, Roy-Contancin L, Feigenbaum P, Kaczorowski GJ, and Garcia ML (1990) Purification and characterization of a unique, potent, peptidyl probe for the high conductance calcium-activated potassium channel from venom of the scorpion *Buthus tamulus*. *J Biol Chem* **265:**11083–11090.

Gauthier KM, Edwards EM, Falck JR, Reddy DS, and Campbell WB (2005) 14,15-epoxyeicosatrienoic acid represents a transferable endothelium-dependent relaxing factor in bovine coronary arteries. *Hypertension* **45:**666–671.

Ghatta S, Nimmagadda D, Xu X, and O'Rourke ST (2006) Large-conductance, calcium-activated potassium channels: structural and functional implications. *Pharmacol Ther* **110:**103–116.

Guo J, Williams DJ, and Ikeda SR (2008) *N*-Arachidonoyl L-serine, a putative endocannabinoid, alters the activation of N-type Ca^{2+} channels in sympathetic neurons. *J Neurophysiol* **100:**1147–1151.

Howlett AC (2005) Cannabinoid receptor signaling. *Handb Exp Pharmacol* **168:**53–79.

Jakab M, Weiger TM, and Hermann A (1997) Ethanol activates maxi Ca^{2+}-activated K^+ channels of clonal pituitary (GH3) cells. *J Membr Biol* **157:**237–245.

Járai Z, Wagner JA, Varga K, Lake KD, Compton DR, Martin BR, Zimmer AM, Bonner TI, Buckley NE, Mezey E, et al. (1999) Cannabinoid-induced mesenteric vasodilation through an endothelial site distinct from CB_1 or CB_2 receptors. *Proc Natl Acad Sci U S A* **96:**14136–14141.

Jiang B, Sun X, Cao K, and Wang R (2002) Endogenous Kv channels in human embryonic kidney (HEK-293) cells. *Mol Cell Biochem* **238:**69–79.

Khan RN, Smith SK, and Ashford MLJ (1998) Contribution of calcium-sensitive potassium channels to NS1619-induced relaxation in human pregnant myometrium. *Hum Reprod* **13:**208–213.

Liu J, Asuncion-Chin M, Liu P, and Dopico AM (2006) CaM kinase II phosphorylation of slo Thr107 regulates activity and ethanol responses of BK channels. *Nat Neurosci* **9:**41–49.

Lu R, Alioua A, Kumar Y, Eghbali M, Stefani E, and Toro L (2006) MaxiK channel partners: physiological impact. *J Physiol* **570:**65–72.

Lukacs V, Thyagarajan B, Varnai P, Balla A, Balla T, and Rohacs T (2007) Dual regulation of TRPV1 by phosphoinositides. *J Neurosci* **27:**7070–7080.

Makriyannis A, Tian X, and Guo J (2005) How lipophilic cannabinergic ligands reach their receptor sites. *Prostaglandins Other Lipid Mediat* **77:**210–218.

Martin G, Puig S, Pietrzykowski A, Zadek P, Emery P, and Treistman S (2004) Somatic localization of a specific large-conductance calcium-activated potassium channel subtype controls compartmentalized ethanol sensitivity in the nucleus accumbens. *J Neurosci* **24:**6563–6572.

Milman G, Maor Y, Abu-Lafi S, Horowitz M, Gallily R, Batkai S, Mo FM, Offertaler L, Pacher P, Kunos G, et al. (2006) *N*-arachidonoyl L-serine, an endocannabinoid-like brain constituent with vasodilatory properties. *Proc Natl Acad Sci U S A* **103:**2428–2433.

Mukhopadhyay S, Chapnick BM, and Howlett AC (2002) Anandamide-induced vasorelaxation in rabbit aortic rings has two components: G protein dependent and independent. *Am J Physiol Heart Circ Physiol* **282:**H2046–H2054.

O'Connell RJ, Yuan C, Johnston LJ, Rinco O, Probodh I, and Treistman SN (2006) Gating and conductance changes in BK(Ca) channels in bilayers are reciprocal. *J Membr Biol* **213:**143–153.

Olesen SP, Munch E, Moldt P, and Drejer J (1994) Selective activation of $Ca^{(2+)}$-dependent K^+ channels by novel benzimidazolone. *Eur J Pharmacol* **251:**53–59.

Oliver D, Lien CC, Soom M, Baukrowitz T, Jonas P, and Fakler B (2004) Functional conversion between A-type and delayed rectifier K^+ channels by membrane lipids. *Science* **304:**265–270.

O'Malley D and Harvey J (2004) Insulin activates native and recombinant large conductance $Ca^{(2+)}$-activated potassium channels via a mitogen-activated protein kinase-dependent process. *Mol Pharmacol* **65:**1352–1363.

Pacher P, Bátkai S, and Kunos G (2006) The endocannabinoid system as an emerging target of pharmacotherapy. *Pharmacol Rev* **58:**389–462.

Plane F, Holland M, Waldron GJ, Garland CJ, and Boyle JP (1997) Evidence that anandamide and EDHF act via different mechanisms in rat isolated mesenteric arteries. *Br J Pharmacol* **121:**1509–1511.

Randall MD, Kendall DA, and O'Sullivan S (2004) The complexities of the cardiovascular actions of cannabinoids. *Br J Pharmacol* **142:**20–26.
Romano MR and Lograno MD (2006) Cannabinoid agonists induce relaxation in the bovine ophthalmic artery: evidences for CB1 receptors, nitric oxide and potassium channels. *Br J Pharmacol* **147:**917–925.
Sade H, Muraki K, Ohya S, Hatano N, and Imaizumi Y (2006) Activation of large-conductance, Ca^{2+}-activated K^+ channels by cannabinoids. *Am J Physiol Cell Physiol* **290:**C77–C86.
Sarker KP and Maruyama I (2003) Anandamide induces cell death independently of cannabinoid receptors or vanilloid receptor 1: possible involvement of lipid rafts. *Cell Mol Life Sci* **60:**1200–1208.
Tarzia G, Duranti A, Tontini A, Piersanti G, Mor M, Rivara S, Plazzi PV, Park C, Kathuria S, and Piomelli D (2003) Design, synthesis, and structure-activity relationships of alkylcarbamic acid aryl esters, a new class of fatty acid amide hydrolase inhibitors. *J Med Chem* **46:**2352–2360.
Varnai P, Thyagarajan B, Rohacs T, and Balla T (2006) Rapidly inducible changes in phosphatidylinositol 4,5-bisphosphate levels influence multiple regulatory functions of the lipid in intact living cells. *J Cell Biol* **175:**377–382.
Watanabe H, Vriens J, Prenen J, Droogmans G, Voets T, and Nilius B (2003) Anandamide and arachidonic acid use epoxyeicosatrienoic acids to activate TRPV4 channels. *Nature* 424:434–438.
Weaver AK, Olsen ML, McFerrin MB, and Sontheimer H (2007) BK channels are linked to inositol 1,4,5-triphosphate receptors via lipid rafts: a novel mechanism for coupling $[Ca(^{2+})](i)$ to ion channel activation. *J Biol Chem* **282:**31558–31568.
Westover EJ, Covey DF, Brockman HL, Brown RE, and Pike LJ (2003) Cholesterol depletion results in sine-specific increase in epidermal growth factor receptor phosphorylation due to membrane level effect. *J Biol Chem* **278:**51125–51133.
White R, Ho WS, Bottrill FE, Ford WR, and Hiley CR (2001) Mechanisms of anandamide-induced vasorelaxation in rat isolated coronary arteries. *Br J Pharmacol* **134:**921–929.
Zhou XB, Arntz C, Kamm S, Motejlek K, Sausbier U, Wang GX, Ruth P, and Korth M (2001) A molecular switch for specific stimulation of the BKCa channel by cGMP and cAMP kinase. *J Biol Chem* **276:**43239–43245.
Zygmunt PM, Petersson J, Andersson DA, Chuang H, Sørgård M, Di Marzo V, Julius D, and Högestätt ED (1999) Vanilloid receptors on sensory nerves mediate the vasodilator action of anandamide. *Nature* **400**:452–457.

Address correspondence to: Grzegorz Godlewski, National Institute on Alcohol Abuse and Alcoholism, 5625 Fishers Lane, Bethesda, MD 20892-9413. E-mail: godlewskig@mail.nih.gov